Acta Oceanol. Sin., 2017, Vol. 36, No. 12, P. 101–110
DOI: 10.1007/s13131-017-1094-z
http://www.hyxb.org.cn
E-mail: hyxbe@263.net

The response of spring phytoplankton assemblage to diluted water and upwelling in the eutrophic Changjiang (Yangtze River) Estuary

SONG Shuqun[1, 2], LI Zhao[1, 2], LI Caiwen[1, 2*], YU Zhiming[1, 2]

[1] CAS Key Laboratory of Marine Ecology and Environmental Sciences, Institute of Oceanology, Chinese Academy of Sciences, Qingdao 266071, China

[2] Laboratory for Marine Ecology and Environmental Science, Qingdao National Laboratory for Marine Science and Technology, Qingdao 266237, China

Received 19 October 2016; accepted 4 May 2017

Abstract

A comprehensive study on the phytoplankton standing stocks, species composition and dominant species in the eutrophic Changjiang (Yangtze River) Estuary (CE) was conducted to reveal the response of phytoplankton assemblage to Changjiang Diluted Water (CDW) and upwelling in the spring. Phytoplankton presented peak standing stocks (13.03 μg/L of chlorophyll *a*, 984.5×10^3 cells/L of phytoplankton abundance) along the surface isohaline of 25. Sixty-six species in 41 genera of Bacillariophyta and 33 species in 19 genera of Pyrrophyta were identified, as well as 5 species in Chlorophyta and Chrysophyta. *Karenia mikimotoi* was the most dominant species, followed by *Prorocentrum dentatum*, *Paralia sulcata*, *Pseudo-nitzschia delicatissima* and *Skeletonema costatum*. A bloom of *K. mikimotoi* was observed in the stratified stations, where the water was characterized by low nitrate, low phosphate, low turbidity, and specific ranges of temperature (18–22 °C) and salinity (27–32). *K. mikimotoi* and *P. dentatum* accumulated densely in the upper layers along the isohaline of 25. *S. costatum* was distributed in the west of the isohaline of 20. Benthonic *P. sulcata* presented high abundance near the bottom, while spread upward at upwelling stations. CDW resulted in overt gradients of salinity, turbidity and nutritional condition, determining the spatial distribution of phytoplankton species. The restricted upwelling resulted in the upward transport of *P. sulcata* and exclusion of *S. costatum*, *K. mikimotoi* and *P. dentatum*. The results suggested that CDW and upwelling were of importance in regulating the structure and distribution of phytoplankton assemblage in the CE and the East China Sea.

Key words: phytoplankton, species composition, algal bloom, upwelling, estuary

Citation: Song Shuqun, Li Zhao, Li Caiwen, Yu Zhiming. 2017. The response of spring phytoplankton assemblage to diluted water and upwelling in the eutrophic Changjiang (Yangtze River) Estuary. Acta Oceanologica Sinica, 36(12): 101–110, doi: 10.1007/s13131-017-1094-z

1 Introduction

The Changjiang (Yangtze River) Estuary (CE) and the adjacent East China Sea (ECS) has been suffering from serious eutrophication in the past decades due to the heavy loading of riverine nutrients (Chai et al., 2006; Li et al., 2007; Zhang et al., 2007). The excessive amounts of nutrients lead to thriving of phytoplankton and subsequent blooms of harmful algal species, mainly dinoflagellates and diatoms (Tang et al., 2006; Zhou et al., 2008). Since the 1980s, the frequency of harmful algal blooms (HABs) in the ECS increased dramatically. Meanwhile, the peak period with frequent HABs has shifted from July–August in the 1980s to May–July in the 1990s, and to May–June during 2000–2004 (Tang et al., 2006). As a subsequent effect of eutrophication, hypoxia had been observed in the study area (Li et al., 2002; Wei et al., 2007; Zhu et al., 2011).

The extension of Changjiang Diluted Water (CDW) influences not only the physicochemical properties but also the phytoplankton assemblage in the CE and the adjacent ECS (Gong et al., 2003; Lie et al., 2003; Wang, 2002; Zhang et al., 2007). Multiple environmental gradients were thereby formed across the shelf. The biomass and productivity of phytoplankton were low near the river mouth due to photosynthetic active radiation (PAR) limitation, then increased gradually with sedimentation of suspended solids, and decreased sharply due to nutrient limitation in the offshore waters (Ning et al., 2004). The structure and distribution of phytoplankton assemblage were subsequently influenced by environmental factors, such as salinity, turbidity, and nutrient structure (He et al., 2007; Luan et al., 2007, 2008; Wang, 2002; Zhao et al., 2013).

Upwelling is of great importance to the ecology of coastal marine ecosystem (Blasco et al., 1980; Cui and Street, 2004; Margalef, 1978a). In the CE and the adjacent ECS, persistent upwelling has been observed in the region of 31°00′–32°00′N, 122°20′–123°10′E from May to August (Zhao, 1993; Zhao et al.,

Foundation item: The National Natural Science Foundation of China-Shandong Joint Fund for Marine Science Research Centers under contract No. U1606404; the Youth Project of Natural Science Foundation of Shandong Province under contract No. ZR2014DQ029; the Youth Project of National Natural Science Foundation of China under contract No. 41606128; the Scientific and Technological Innovation Project of Qingdao National Laboratory for Marine Science and Technology under contract Nos 2016ASKJ02 and 2015ASKJ02; the Aoshan Talents Program of Qingdao National Laboratory for Marine Science and Technology under contract No. 2015ASTP.
*Corresponding author, E-mail: cwli@qdio.ac.cn

2001). The spring upwelling was characterized by low temperature (16–21°C), high salinity (24–33) and low dissolved oxygen (2.5–6.0 mg/L) in the upper 10 m of the water column (Pei et al., 2009). The summer upwelling was weaker in intensity and smaller in geographical scale, thus the upper 10 m of the water column was strongly influenced by turbid CDW instead of upwelling (Pei et al., 2009).

The phytoplankton assemblage and its association to nutrient input had been comprehensive studied in the CE and the adjacent ECS since the 1980s (Zhou et al., 2006). While, there is little information on the response of phytoplankton assemblage to the upwelling in the area. Thus, in the present study, we carried out a multi-discipline survey in the CE and the adjacent ECS during spring to study the abundance, distribution and species composition of marine phytoplankton and their correlation with the major environmental factors, and to further reveal the influence of CDW and upwelling on the phytoplankton assemblage in the eutrophic estuary. The underlying hypothesis is that the phytoplankton assemblage can be significantly influenced by the coupling effect of CDW and restricted upwelling in the area.

2 Methods

2.1 *Sampling and analysis*

Sampling was carried out in the CE and the adjacent ECS (30.5°–32.5°N, 121.0°–123.5°E). Twenty-five stations along four transects were investigated during spring (22–28 May 2012) (Fig. 1).

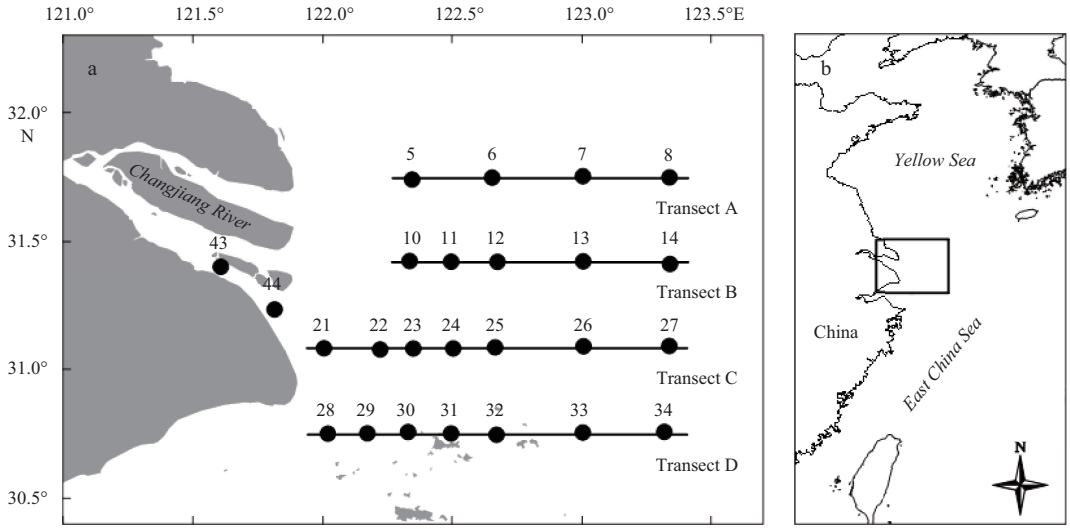

Fig. 1. Sampling stations in the CE (a) and the adjacent ECS (b).

Salinity and temperature were monitored by CTD probes (SBE 911, Sea-Bird Electronics, USA). Turbidity was measured with the OBS3 sensor according to the optical backscatter method. Seawater samples were collected from standard depths (0 m, 5 m, 10 m, 20 m, 30 m, 50 m, 2 m above bottom) using 12-L Niskin bottles. Seawater samples were filtered through 0.45 μm acetate fiber membrane for analysis of inorganic nutrients (nitrate, nitrite, ammonium, phosphate and silicate), which were measured with a Continuous Flow Analyzer (San^{++}, SKALAR, Netherland). Chlorophyll *a* (Chl *a*) samples were collected by filtering seawater onto GF/F filters under low vacuum pressure (<0.04 MPa) and stored at –20°C in the dark. Chl *a* samples were extracted with 90% acetone overnight at 4°C in the dark. Then, Chl *a* concentrations were measured with a fluorometer (Trilogy, Turner Design, USA) by the fluorometric technique (Strickland and Parsons, 1972).

For analysis of phytoplankton assemblage, Aliquots of 250 mL seawater samples were collected at the above-mentioned depths, then preserved immediately with buffered formalin (final concentration 2%) and kept in plastic bottles at room temperature until they were analyzed. Following the methodology described by Utermöhl (1958), 10–25 mL of the subsamples were settled in a Hydro-bios chamber for 24 h, then counted using an inverted light microscope (IX71, Olympus, Japan). Identification and enumeration of taxa were carried out at 200× or 400× magnification, and species nomenclature was validated according to Tomas (1997).

2.2 *Data analysis*

The dominances of phytoplankton species were described by McNaughton index (Y): $Y=f_i\ n_i/N$, where N is the sum of cell abundance for all species, n_i is the sum of cell abundance for species i in all samples, f_i is the occurrence frequency for species i in all samples.

The Detrended Correspondence Analysis (DCA) of phytoplankton data indicated that the length of gradient was less than 3 at Axes 1. Thus, the Redundancy Analysis (RDA) was performed with the abundances of major phytoplankton species and environmental factors in the water column. The major phytoplankton species were chosen based on two criteria, appearing at more than three stations and exceeding 1% of the total phytoplankton abundance at the least one station. The environmental factors included salinity, temperature, turbidity, inorganic nutrients and the sampling depth. For data normality, all values of environmental factors except sampling depth were transformed by lg$x$, and the values of phytoplankton abundance were transformed by lg(x+1). Both DCA and RDA were carried out by the Canoco software for Windows (Version 4.5, Plant Research International, Netherland).

3 Results

3.1 *Variations of major environmental factors*

Due to the large amount of freshwater discharge from the

Changjiang River, the surface salinity was lower than 5 near the river mouth. As freshwater mixed with saline water, salinity increased dramatically towards the offshore direction. The low-salinity tongue indicated the southeastward expansion of CDW (Fig. 2a). The sea surface temperature ranged from 18.4 to 24.5°C. It was relatively low in the middle of the study area (Fig. 2b). The surface turbidity and nutrient concentrations were extremely high near the river mouth, with maximum value of 334.58 RFU for turbidity, 78.44 μmol/L for nitrate, 1.63 μmol/L for phosphate and 72.69 μmol/L for silicate. Generally, there were clear decreasing patterns of turbidity, nitrate, phosphate and silicate along with expansion of CDW (Figs 2c–f).

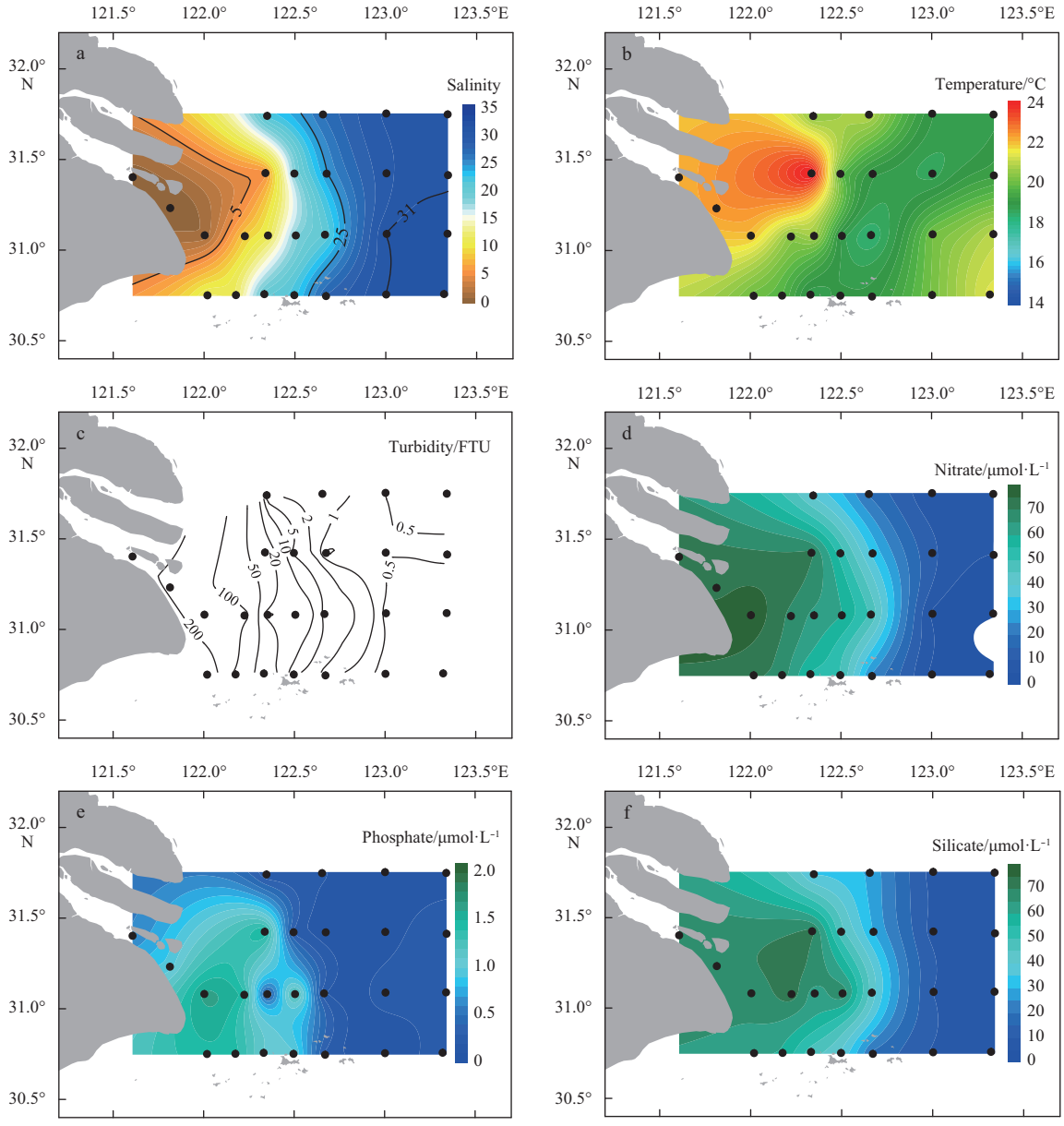

Fig. 2. Horizontal distributions of salinity, temperature, turbidity and nutrients in the surface water.

Strong stratification of water column was observed in Transects A and B (Figs 3a, b, e and f). The CDW characterized by lower salinity and higher temperature was confined to the upper layers, and became thinner when further mixing with saline ambient water. Isotherms rose from the bottom toward the surface in Transect C (between 16.8°C and 19.2°C) and Transect D (between 18.0°C and 19.2°C) (Figs 3g and h). The 16.8°C line extended from ~30 m to ~10 m around Sta. 25, and the 18.0°C line extended from ~20 m to ~10 m around Sta. 32, and the 19.2°C line extended from ~15 m to the surface in both transects. No obvious concavity of isohalines was observed in Transects C and D (Figs 3c and d).

The concavity of isotherms was significant in Transect C. Thus, the turbidity and nutrient concentrations along Transect C were further evaluated with vertical profiles. The turbidity increased with depth vertically, and decreased toward the offshore direction in the upper layers. Its isolines were slightly concave near Stas 24 and 25 (Fig. 4a). The concentrations of nitrate and silicate decreased with salinity as the CDW expanded eastward (Figs 3c, 4b and 4d). The isolines of phosphate concentration showed clear concavity at Sta. 24, where the surface phosphate concentrations were significantly higher than other inshore sta-

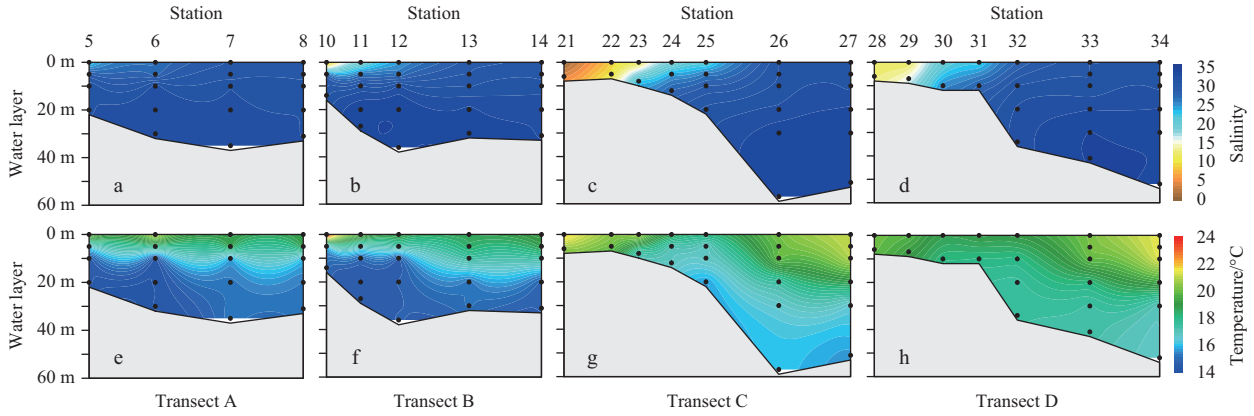

Fig. 3. Vertical profiles of salinity and temperature in Transects A, B, C, and D.

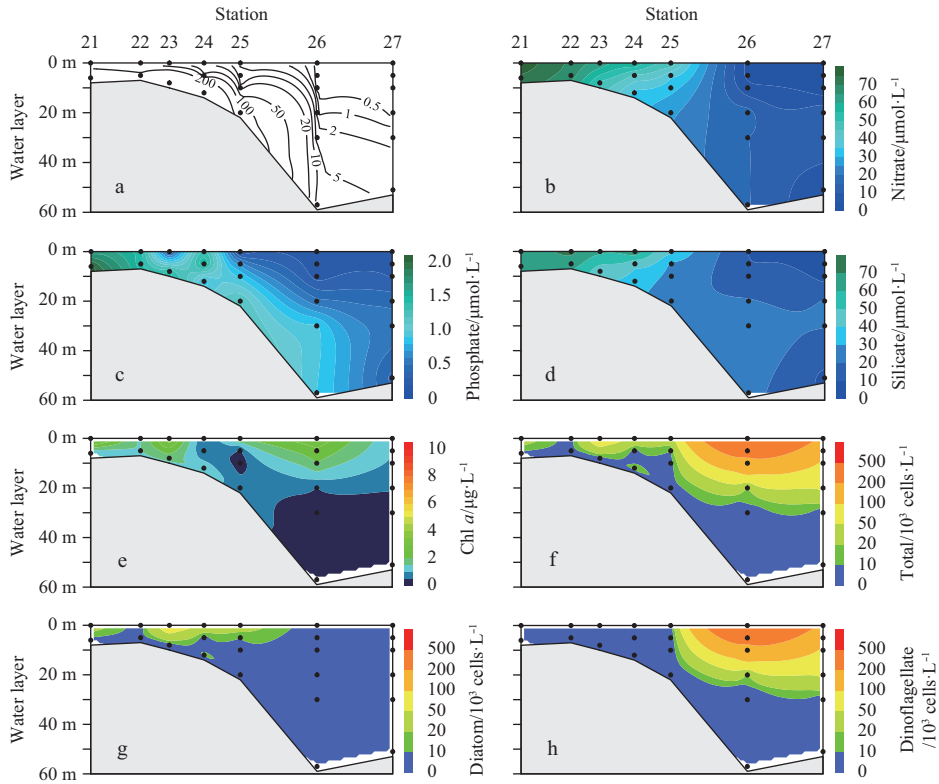

Fig. 4. Vertical profiles of turbidity, nutrient concentrations, Chl *a* concentration and phytoplankton abundance in Transect C.

tions (Figs 2e and 4c). The concave isolines of temperature, turbidity and phosphate indicated the upwelling occurring around 31°05′N, 122°30′E in the spring of 2012.

3.2 *Chl a and phytoplankton abundance*

The Chl *a* concentrations were highly variable both horizontally and vertically. They ranged from 0.09 to 13.03 μg/L with average of 1.19 μg/L. The surface Chl *a* concentrations were lower inside the river mouth, and increased toward the offshore direction (Fig. 5a). Two patches with higher Chl *a* concentration were located between 122.50°E and 123.00°E. One was around Sta. 6, and another one was around Sta. 32. Vertically, the Chl *a* concentrated at the surface and 5 m layer, and the overall pattern of Chl *a* concentrations decreased gradually with depth (Fig. 6a). In Transect C, Chl *a* concentrations were higher in the upper layers of those non-upwelling stations, while there was a low Chl *a* tongue spread from the bottom to the upper layers at the upwelling stations (Fig. 4e).

The phytoplankton abundances ranged from 0.8×10^3 to 984.5×10^3 cells/L with average of 68.5×10^3 cells/L. Similar to the distribution of surface Chl *a*, surface phytoplankton presented two patches with higher abundance around Stas 6 and 32, respectively (Fig. 5b). In the surface layer, the abundance of dinoflagellate ranged from 0 to 922.0×10^3 cells/L, and the abundance of diatom ranged from 0.04×10^3 to 204.5×10^3 cells/L. Dinoflagellates and diatoms dominated the sampling stations alternately during the survey (Figs 5c and d). The mean abundances of diatoms were 28.30×10^3 cells/L at surface, 17.21×10^3 cells/L at 5 m depth, and about 10×10^3 cells/L at layers below 5 m. The mean abundances of dinoflagellates were 113.98×10^3 cells/L at surface,

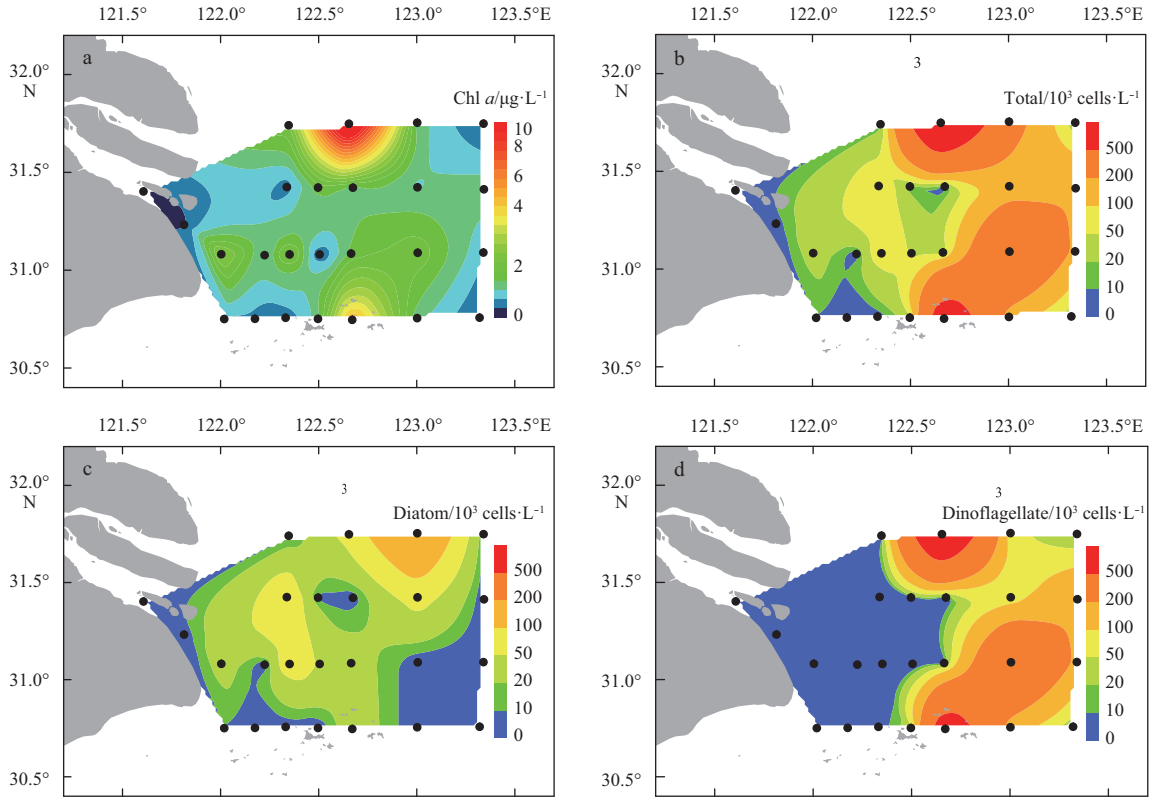

Fig. 5. Distributions of Chl *a*, and phytoplankton, diatom and dinoflagellate abundance in the surface water.

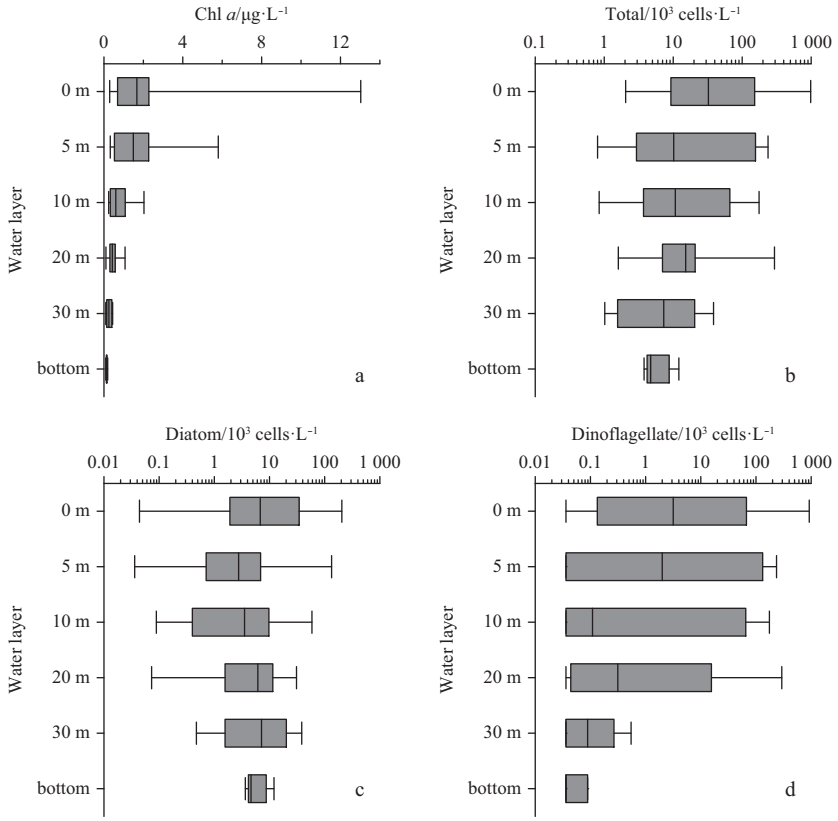

Fig. 6. Vertical distributions of Chl *a* and phytoplankton, diatom and dinoflagellate abundance. The black lines inside the boxes denote the median value, the bottom and top of the boxes represent the lower and upper quartile of the data respectively. The whiskers extending from the boxes indicate the positions of the maximum and minimum in the data.

56.25×10^3 cells/L at 5 m layer, 30.01×10^3 cells/L at 10 m layer, 27.54×10^3 cells/L at 20 m layer, and less than 1×10^3 cells/L at 30 m layer and bottom. Generally, the maximum abundance of both diatoms and dinoflagellates appeared at the surface (Figs 6c and d). The median abundance of diatoms at the surface layer was the highest among the six layers; however, the differences were not significant. The median abundance of dinoflagellates at the surface layer and 5 m layer were much higher than layers below 5 m. In Transect C, diatoms dominated the phytoplankton assemblage in the upper layers (above 10 m) from the river mouth to upwelling area (Fig. 4g), whereas dinoflagellates dominated the phytoplankton assemblage from the surface to 30 m layer to the east of the upwelling area (Fig. 4h).

3.3 *Species composition and distribution of dominant species*

Altogether 107 taxa were identified in the study area, diatoms and dinoflagellates were the dominant groups. Sixty-six species belonged to 41 genera of diatoms (Bacillariophyta), and 33 species belonged to 19 genera of dinoflagellates (Pyrrophyta). Other species belonged to three genera of green algae (Chlorophyta) and one genus of silicoflagellates (Chrysophyta). Most of these species were neritic or cosmopolitan, and a few species were brackish, such as *Skeletonema costatum*, *Bleakeleya notate* and *Scrippsiella trochoidea*.

The top 10 dominant species of phytoplankton were listed in the Table 1. *Karenia mikimotoi* was the most dominant species, followed by *Prorocentrum dentatum* (also known as *Proro-*

Table 1. Top 10 dominant species of phytoplankton assemblage

Species	Phylum	f_i	n_i/N	Y
Karenia mikimotoi	dinoflagelltates	0.559	0.631	0.352 5
Prorocentrum dentatum	dinoflagelltates	0.419	0.114	0.047 9
Paralia sulcata	diatoms	0.688	0.051	0.035 1
Pseudo-nitzschia delicatissima	diatoms	0.398	0.081	0.032 1
Skeletonema costatum	diatoms	0.226	0.047	0.010 6
Noctiluca scintillans	dinoflagelltates	0.430	0.006	0.002 5
Chaetoceros sp.	diatoms	0.215	0.007	0.001 6
Ceratium lineatum	dinoflagelltates	0.376	0.003	0.001 2
Rhizosolenia setigera	diatoms	0.237	0.005	0.001 2
Scrippsiella trochoidea	dinoflagelltates	0.409	0.003	0.001 1

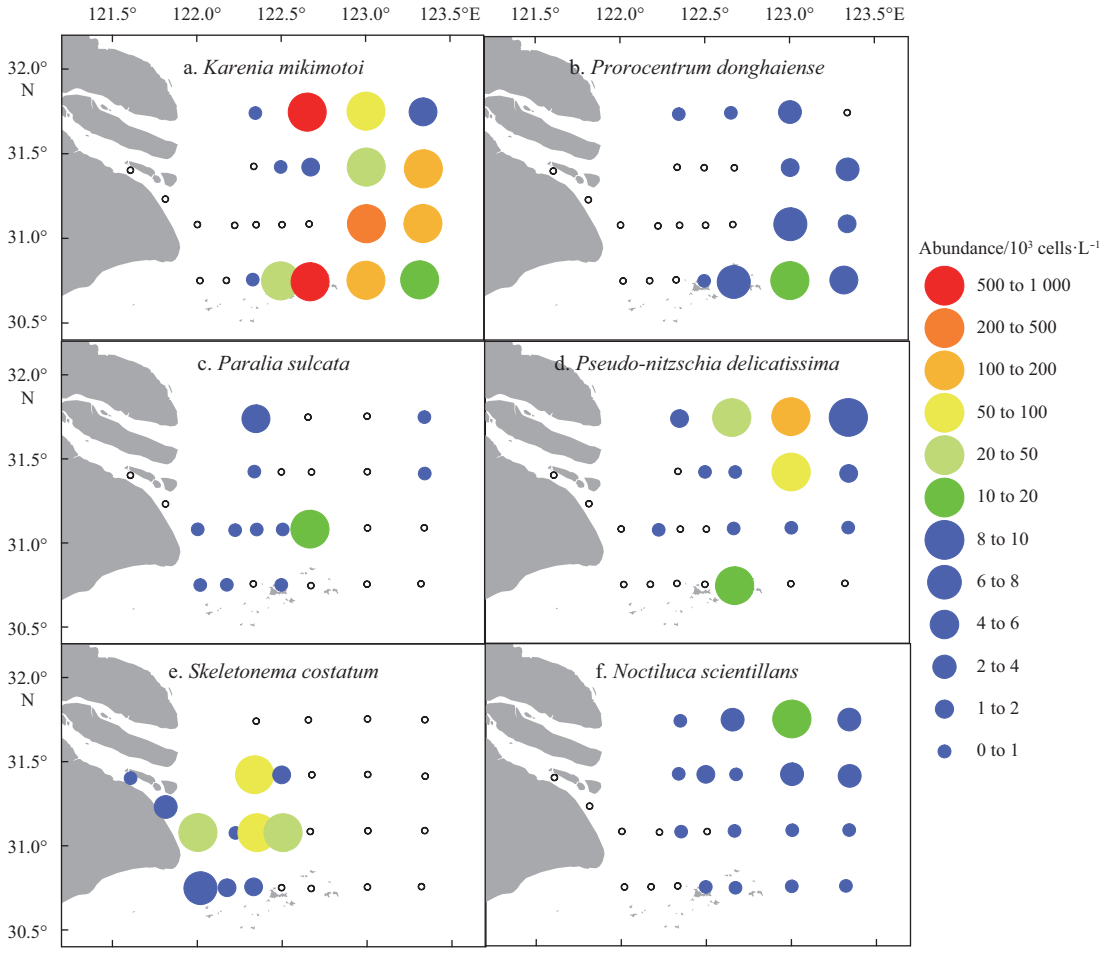

Fig. 7. Horizontal distributions of the abundance of dominant species in the surface water. The color and size of dots represent the abundance of dominant species.

centrum donghaiense). *K. mikimotoi* and *P. dentatum* accounted for more than 70% of total phytoplankton abundance. *P. sulcata* had the maximum f_i, and was the most dominant diatom species. All the dominant diatoms listed in Table 1 were chain-forming species.

The horizontal distribution and vertical profile of dominant species were shown in Fig. 7 and Fig. 8. *K. mikimotoi* was mainly distributed in the east of the study area, and accumulated densely in the upper layers along the isohaline of 25 (Figs 2a and 7a). *P. dentatum* showed similar distribution pattern as to *K. mikimotoi*, but with different locality of high-abundance patches (Fig. 7b). The benthonic diatom *P. sulcata* was widely distributed in the bottom at all stations, while only appeared in the surface layer of inshore stations and offshore Stas 8 and 14. It presented higher abundance in the surface layer of upwelling stations (Fig. 7c). *P. delicatissima* was mainly observed in the surface of the offshore waters, while rarely found at inshore stations (Fig. 7d). *S. costatum* was distributed in the low-salinity (<25) water, and showed higher abundance near the river mouth (Figs 2a and 7e). *N. scintillans* was widely dispersed in the upper layers, and its high-abundance patches coincided with that of *P. delicatissima* (Figs 7d and f).

K. mikimotoi and *P. dentatum* presented higher abundance at Stas 6, 26, 27, 32, 33 and 34 (Fig. 9). Thermocline and halocline appeared between 5 m and 30 m. *K. mikimotoi* and *P. dentatum* accumulated densely in the upper mixed layer, characterized with low turbidity, low concentrations of nitrate and phosphate, specific range of temperature (18–22°C) and salinity (27–32). In addition, the maximum abundance of *K. mikimotoi* and *P. dentatum* appeared at different depths of the six stations. They arose in the surface layer or 5 m layer in the daytime, while sank to the 20 m layer in the night.

3.4 *Effects of environmental factors on phytoplankton composition*

The correlation between phytoplankton species and environmental variables determining the spatial variability of phytoplankton composition were shown in the bi-plot of RDA (Fig. 10). The right section represents the offshore waters characterized by high salinity, temperature and ammonium. The upper left section represents the inshore upper layer water characterized by high nitrate, phosphate and silicate and low salinity. The lower left section represents the deep water characterized by low temperature. The abundances of all the dinoflagellate and some diatoms (such as *P. delicatissima* and *R. setigera*) positively correlated with salinity, and negatively correlated with major nutrients except ammonium. The *K. mikimotoi* abundance and *P. dentatum* abundance showed significantly positive correlation

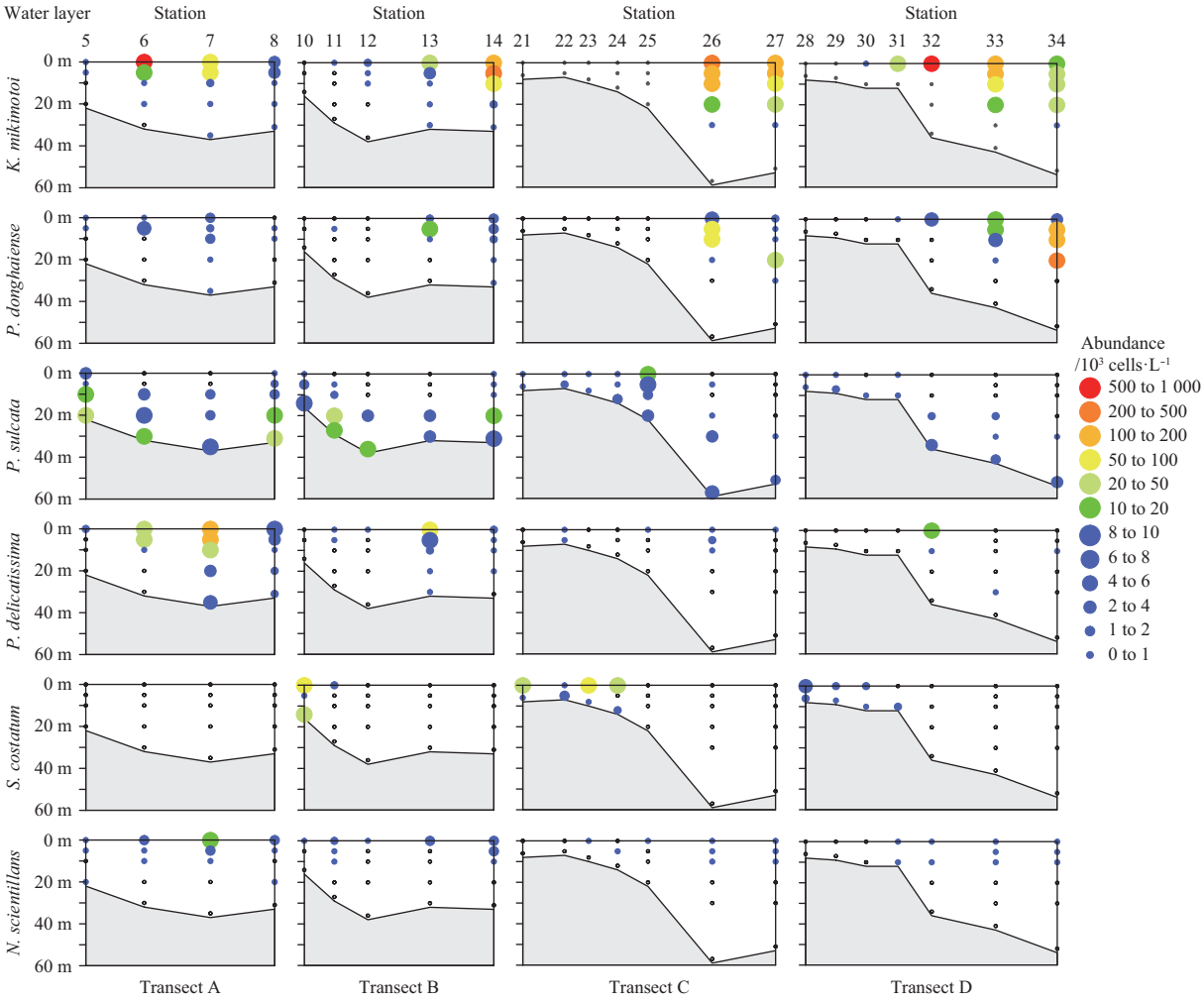

Fig. 8. Vertical profiles of the abundance of dominant species in Transects A, B, C and D. The color and size of dots represent the abundance of dominant species.

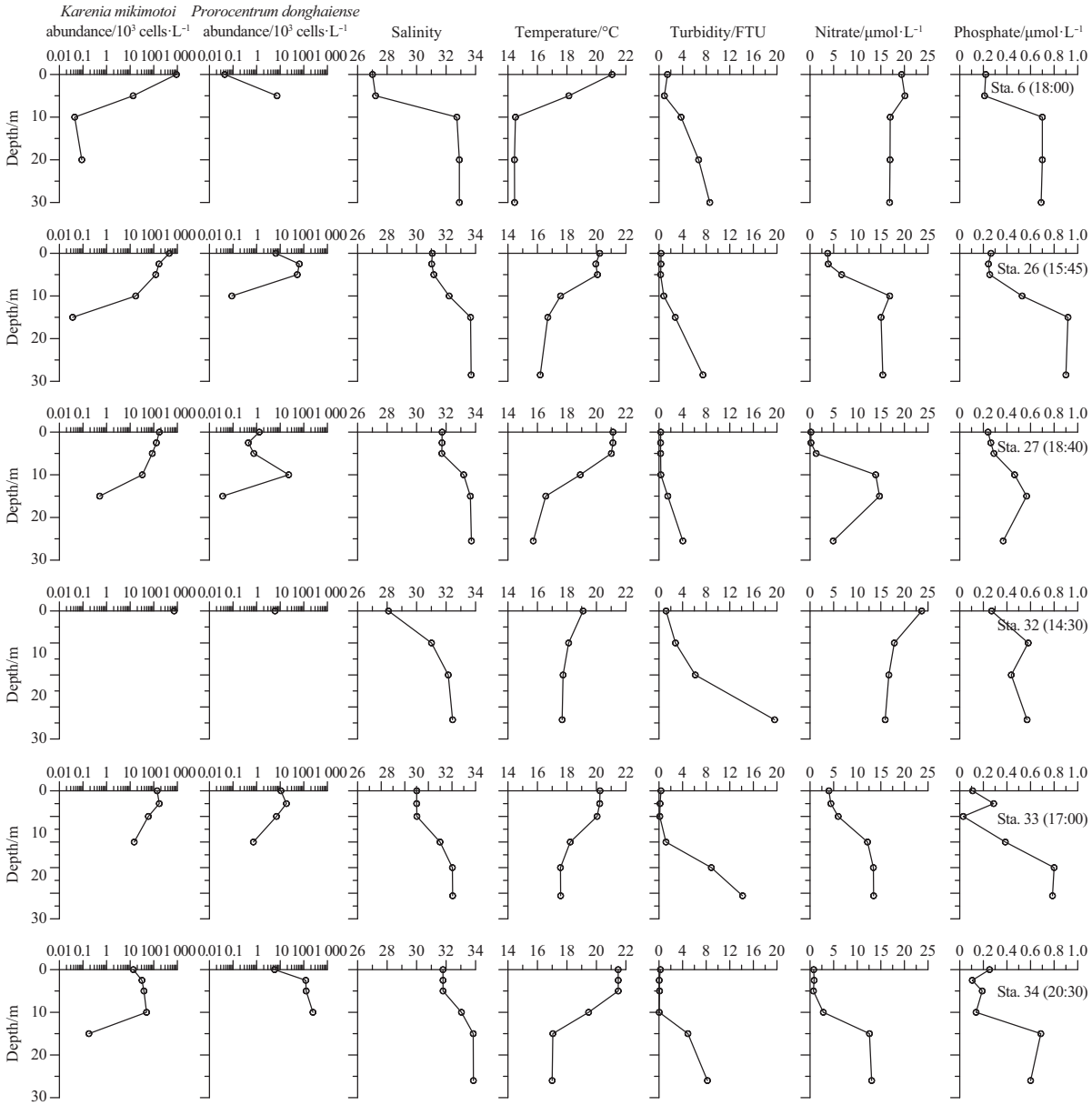

Fig. 9. Vertical profiles of the abundances of *Karenia mikimotoi* and *Prorocentrum dentatum*, salinity, temperature, turbidity, and the concentrations of nitrate and phosphate at Stas 6, 26, 27, 32, 33 and 34. The sampling time-points were shown in the brackets.

with ammonium and temperature. The abundances of brackish diatoms and green algae showed significantly positive correlation with nitrate, phosphate and silicate, and negative correlation with salinity. The *P. sulcata* abundance correlated positively with nitrite and sampling depth, while negatively with temperature. Furthermore, there was no significant correlation between the *P. sulcata* abundance and the other nutrients and salinity.

4 Discussion

With the expansion of CDW, multiple environmental gradients formed outside the river mouth, and resulted in alteration of phytoplankton assemblage. Salinity can demarcate the distribution of phytoplankton species in the CE (He et al., 2007; Luan et al., 2007, 2008; Zhao et al., 2013). Green algae *Scenedesmus quadricauda* and *Pediastrum simplex* correlated negatively with salinity, and was distributed inside the isohaline of 5. *S. costatum* was distributed inside the isohaline of 20, as its optimal salinity ranges from 14 to 23 (Li et al., 2005). Turbulence can affect the species composition of phytoplankton assemblage. Dinoflagellates were not able to survive in highly turbulent water, and a dinoflagellate to diatom community shift would occur when water turbulence level increased (Margalef, 1978b). Thus, dinoflagellates mainly appeared at stratified stations rather than well-mixed stations. Moreover, silicate was able to influence the species composition of phytoplankton assemblage. Diatoms became dominant when silicate concentration was higher than 2 μmol/L and other nutrients were sufficient (Egge, 1998). In the present study, dinoflagellates were more abundant than diatoms at most stations. Whereas the minimum concentration of silicate was 5.46 μmol/L, diatoms could not be limited by silicate. Phosphate might be the limiting factor in the growth of diatoms (Egge, 1998; Pu et al., 2001).

The spatial distribution of phytoplankton standing stocks, i.e., Chl *a* and cell abundance, were also affected by the CDW. Due to

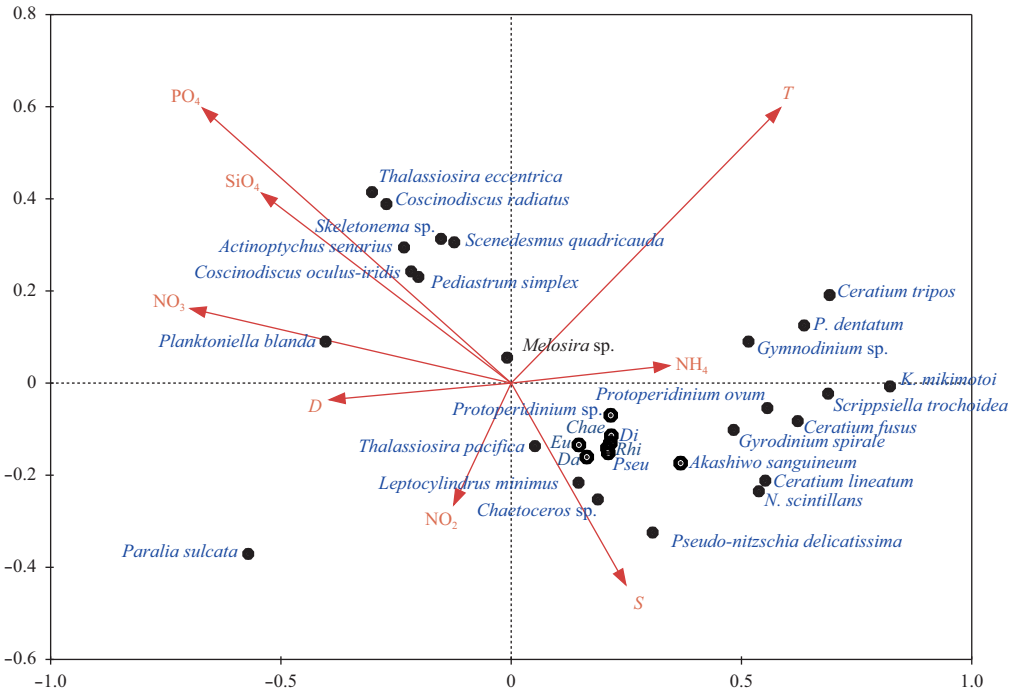

Fig. 10. Redundancy analysis (RDA) of the major phytoplankton species and environmental factors. *T* is temperature, *S* salinity, NO_3 nitrate, NO_2 nitrite, NH_4 ammonium, PO_4 phosphate, SiO_4 silicate, and *D* sampling depth. *Chae* represents *Chaetoceros lorenzianus*, *Da Dactyliosolen fragilissimus*, *Eu Eucampia cornuta*, *Pseu Pseudo-nitzschia pungens*, *Rhi Rhizosolenia setigera*, and *Di Dictyocha speculum*.

the sediment resuspension processes caused by strong water mixing, the turbidity was extremely high around the river mouth (Li and Zhang, 1998). PAR limited the growth of phytoplankton in the upper estuary; thereby phytoplankton presented low standing stocks near the river mouth (Ning et al., 2004; Shen, 1991). As CDW spreading, both Chl *a* and cell abundance increased with the drop of turbidity, and reached maximum abundance along the isohaline of 25. In the offshore waters, Chl *a* and cell abundance decreased along with the depletion of nutrients, because the low concentrations of nutrients limited the growth of phytoplankton (Gong et al., 2003; Ning et al., 2004). Generally, phytoplankton standing stocks accumulated in the upper layer. However, the patches with high standing stocks could expand downward as a result of decreasing turbidity in the offshore waters.

A typical upwelling, indicated by concave isolines of sea temperature, salinity, turbidity and phosphate in Transect C, was observed in the vicinity of Stas 24 and 25. However, this upwelling was weaker in intensity and smaller in geographical area compared to the spring upwelling observed in 2004 (Pei et al., 2009). The temperature difference between the surface and upwelled water was about 2°C, lower than that in the spring of 2004 (3°C). Additionally, the surface salinity in the upwelling area of 2012 was 3–5 lower than that of 2004. The increase of phosphate and the decrease of turbidity did not lead to the increase of Chl *a* and phytoplankton abundance in the upper layer of upwell station. Phytoplankton growth could be limited by the low temperature and the low concentrations of nitrate and silicate in upwelled seawaters (Zhao et al., 2001). Furthermore, the species composition was significantly influenced by the upwelling. Benthonic *P. sulcata* was transported upward and presented higher abundance at the surface layer of Sta. 25. While *S. costatum*, *K. mikimotoi* and *P. dentatum* were not found at upwelling stations despite they presented high abundance at nearby stations. The dispersion of *K. mikimotoi* and *P. dentatum* was interdicted by the high turbulence level in the upwelling area.

HAB has been a seasonal recurrent phenomenon coupled with eutrophication in the CE and the adjacent ECS in recent decades (Tang et al., 2006). *P. dentatum* was the most popular HAB dinoflagellate, followed by *K. mikimotoi* (Shen et al., 2011). A bloom of *K. mikimotoi* was observed at Sta. 7. The maximum abundance of *K. mikimotoi* was 909.9×10^3 cells/L, and *P. dentatum* presented maximum abundance of 243.3×10^3 cells/L. Water stratification was considered to be the essential physical condition that dinoflagellates require to bloom (Smayda, 1997). Temperature and salinity were of importance to regulate the formation of dinoflagellate blooms (Chen et al., 2005; Long and Du, 2005; Wang and Huang, 2003). In addition, Low turbidity and low concentrations of nitrate and phosphate also favored the growth of *K. mikimotoi* and *P. dentatum* (Wang and Huang, 2003). Both *K. mikimotoi* and *P. dentatum* accumulated in the upper mixed layer, where the temperature and salinity were consistent with the optimal temperature and salinity range reported in the literatures (Chen et al., 2005; Long and Du, 2005; Wang and Huang, 2003). Moreover, the turbidity and concentrations of nitrate and phosphate were at low levels in the upper mixed layer. Because dinoflagellates can migrate vertically (Estrada and Berdalet, 1998; Gentien et al., 2007; Wang and Huang, 2003), the depths of the maximum abundance of *K. mikimotoi* and *P. dentatum* varied diurnally. Furthermore, *P. dentatum* can accumulate at the intermediate depth before bloom then migrate upward as the population multiplied (Chen et al., 2006).

5 Conclusions

The CDW induced sharp environmental gradients, such as salinity, turbidity and nutritional condition, thus influenced the

spatial distribution of phytoplankton in the CE and the adjacent ECS. Both Chl *a* concentration and phytoplankton abundance presented maxima within the upper mixed layers along the surface isohaline of 25. Furthermore, the composition of phytoplankton assemblage varied along the pathway of CDW, and the dominant species showed distinctive distribution patterns according to their inherent environmental adaptation. The restricted upwelling influenced the composition of phytoplankton assemblage by causing upward transport of *P. sulcata* and exclusion of *S. costatum*, *K. mikimotoi* and *P. dentatum*. Compared with CDW, the influence of upwelling on phytoplankton assemblage was exerted in smaller scope. Low nitrate, low phosphate, low turbidity, and specific ranges of temperature (18–22°C) and salinity (27–32) could favor the formation of *K. mikimotoi* bloom.

Acknowledgements

The authors thank the colleagues from Key Laboratory of Marine Ecology and Environmental Sciences for their assistance in field and laboratory work.

References

Blasco D, Estrada M, Jones B. 1980. Relationship between the phytoplankton distribution and composition and the hydrography in the northwest African upwelling region near Cabo Corbeiro. Deep-Sea Res Part I, 27A(10): 799–821

Chai Chao, Yu Zhiming, Song Xiuxian, et al. 2006. The status and characteristics of eutrophication in the Yangtze River (Changjiang) Estuary and the adjacent East China Sea, China. Hydrobiologia, 563(1): 313–328

Chen Hanlin, Lv Songhui, Zhang Chuansong, et al. 2006. A survey on the red tide of *Prorocentrum donghaiense* in East China Sea, 2004. Ecol Sci (in Chinese), 25(3): 226–230

Chen Bingzhang, Wang Zongling, Zhu Mingyuan, et al. 2005. Effects of temperature and salinity on growth of *Prorocentrum dentatum* and comparisons between growths of *Prorocentrum dentatum* and *Skeletonema costatum*. Adv Mar Sci (in Chinese), 23(1): 60–64

Cui Anqing, Street R L. 2004. Large-eddy simulation of coastal upwelling flow. Environ Fluid Mech, 4(2): 197–223

Egge J K. 1998. Are diatoms poor competitors at low phosphate concentrations?. J Mar Syst, 16(3–4): 191–198

Estrada M, Berdalet E. 1998. Phytoplankton in a turbulent world. Sci Mar, 61(S1): 125–140

Gentien P, Lunven M, Lazure P, et al. 2007. Motility and autotoxicity in *Karenia mikimotoi* (Dinophyceae). Philos Trans R Soc Lond B Biol Sci, 362(1487): 1937–1946

Gong G C, Wen Y H, Wang B W, et al. 2003. Seasonal variation of chlorophyll *a* concentration, primary production and environmental conditions in the subtropical East China Sea. Deep-Sea Res Part II, 50(6–7): 1219–1236

He Qing, Sun Jun, Luan Qingshan, et al. 2007. Phytoplankton assemblage in Yangtze River Estuary and its adjacent waters in winter time. Chin J Appl Ecol (in Chinese), 18(11): 2559–2566

Li Maotian, Xu Kaiqin, Watanabe M, et al. 2007. Long-term variations in dissolved silicate, nitrogen, and phosphorus flux from the Yangtze River into the East China Sea and impacts on estuarine ecosystem. Estuar Coast Shelf Sci, 71(1–2): 3–12

Li Jiufa, Zhang Chen. 1998. Sediment resuspension and implications for turbidity maximum in the Changjiang Estuary. Mar Geol, 148(3–4): 117–124

Li Daoji, Zhang Jing, Huang Daji, et al. 2002. Oxygen depletion off the Changjiang (Yangtze River) Estuary. Sci China Ser D, 45(12): 1137–1146

Li Jintao, Zhao Weihong, Yang Dengfeng, et al. 2005. Effect of turbid water in Changjiang (Yangtze) Estuary on the growth of *Skeletonema costatum*. Mar Sci (in Chinese), 29(1): 34–37

Lie H J, Cho C H, Lee J H, et al. 2003. Structure and eastward extension of the Changjiang River plume in the East China Sea. J Geophys Res, 108(C3): 3077

Long Hua, Du Qi. 2005. Primary research on *Karenia mikimotoi* bloom in Fujian coast. J Fujian Fish (in Chinese), (107): 22–25

Luan Qingshan, Sun Jun, Song Shuqun, et al. 2007. Canonical correspondence analysis of summer phytoplankton community and its environment in the Yangtze River Estuary, China. J Plant Ecol (in Chinese), 31(3): 445–450

Luan Qingshan, Sun Jun, Song Shuqun, et al. 2008. Phytoplankton assemblage in Changjiang Estuary and its adjacent waters in autumn, 2004. Adv Mar Sci (in Chinese), 26(3): 364–371

Margalef R. 1978a. Phytoplankton communities in upwelling areas: the example of NW Africa. Oecol Aquat, 3: 97–132

Margalef R. 1978b. Life-forms of phytoplankton as survival alternatives in an unstable environment. Oceanol Acta, 1(4): 493–509

Ning Xiuren, Shi Junxian, Cai Yuming, et al. 2004. Biological productivity front in the Changjiang Estuary and the Hangzhou Bay and its ecological effects. Acta Oceanol Sin (in Chinese), 26(6): 96–106

Pei Shaofeng, Shen Zhiliang, Laws E A. 2009. Nutrient dynamics in the upwelling area of Changjiang (Yangtze River) estuary. J Coast Res, 25(3): 569–580

Pu Xinming, Wu Yulin, Zhang Yongshan. 2001. Nutrient limitation of phytoplankton in the Changjiang Estuary II. Condition of nutrient limitation in spring. Acta Oceanol Sin (in Chinese), 23(3): 57–65

Shen Zhiliang. 1991. A study on the effects of the Three Gorge Project on the distributions and changes of the nutrients in the Changjiang River estuary. Oceanol Limnol Sin (in Chinese), 22(6): 540–546

Shen Li, Xu Huiping, Guo Xulin, et al. 2011. Characteristics of large-scale harmful algal blooms (HABs) in the Yangtze River estuary and the adjacent East China Sea (ECS) from 2000 to 2010. J Environ Prot, 2(10): 1285–1294

Smayda T J. 1997. Harmful algal blooms: their ecophysiology and general relevance to phytoplankton blooms in the sea. Limnol Oceanogr, 42: 1137–1153

Strickland J D H, Parsons T R. 1972. A Practical Handbook of Seawater Analysis. Ottawa: Fisheries Research Board of Canada, 167: 201–206

Tang Danling, Di Baoping, Wei Guifeng, et al. 2006. Spatial, seasonal and species variations of harmful algal blooms in the South Yellow Sea and East China Sea. Hydrobiologia, 568(1): 245–253

Tomas C R. 1997. Identifying Marine Phytoplankton. New York: Academic Press, 1–858

Utermöhl H. 1958. Zur Vervolkommung der quantitativen Phytoplankton-Methodik. Mitt Int Ver Theor Angew Limnol (in German), 9: 1–38

Wang Jinhui. 2002. Phytoplankton communities in three distinct ecotypes of the Changjiang Estuary. J Ocean Univ Qingdao (in Chinese), 32(3): 422–428

Wang Jinhui, Huang Xiuqing. 2003. Ecological characteristics of *Prorocentrum dentatum* and the cause of harmful algal bloom formation in China Sea. Chin J Appl Ecol (in Chinese), 14(7): 1065–1069

Wei Hao, He Yunchang, Li Qingji, et al. 2007. Summer hypoxia adjacent to the Changjiang Estuary. J Mar Syst, 67(3–4): 292–303

Zhang Jing, Liu Sumei, Ren Jingling, et al. 2007. Nutrient gradients from the eutrophic Changjiang (Yangtze River) Estuary to the oligotrophic Kuroshio waters and re-evaluation of budgets for the East China Sea Shelf. Prog Oceanogr, 74(4): 449–478

Zhao Baoren. 1993. Upwelling phenomenon off the Changjiang Estuary. Haiyang Xuebao (in Chinese), 15(2): 108–114

Zhao Baoren, Ren Guangfa, Cao Deming, et al. 2001. Characteristics of the ecological environment in upwelling area adjacent to the Changjiang River estuary. Oceanol Limnol Sin (in Chinese), 32(3): 327–333

Zhao Ran, Sun Jun, Song Shuqun. 2013. Phytoplankton in the Yangtze River Estuary and its adjacent waters in spring 2006. Mar Sci Bull (in Chinese), 32(4): 421–428

Zhou Mingjiang, Shen Zhiliang, Yu Rencheng. 2008. Responses of a coastal phytoplankton community to increased nutrient input from the Changjiang (Yangtze) River. Cont Shelf Res, 28(12): 1483–1489

Zhu Zhuoyi, Zhang Jing, Wu Ying, et al. 2011. Hypoxia off the Changjiang (Yangtze River) Estuary: oxygen depletion and organic matter decomposition. Mar Chem, 125(1–4): 108–116